



HAL
open science

Study of the effect of gas pressure and catalyst droplets number density on silicon nanowires growth, tapering, and gold coverage

W.H. Chen, Rodrigue Lardé, E. Cadel, T. Xu, B. Grandidier, J.P. Nys, D. Stievenard, Philippe Pareige

► To cite this version:

W.H. Chen, Rodrigue Lardé, E. Cadel, T. Xu, B. Grandidier, et al.. Study of the effect of gas pressure and catalyst droplets number density on silicon nanowires growth, tapering, and gold coverage. *Journal of Applied Physics*, 2010, 107 (8), pp.0849028. 10.1063/1.3359648 . hal-00549438

HAL Id: hal-00549438

<https://hal.science/hal-00549438v1>

Submitted on 25 May 2022

HAL is a multi-disciplinary open access archive for the deposit and dissemination of scientific research documents, whether they are published or not. The documents may come from teaching and research institutions in France or abroad, or from public or private research centers.

L'archive ouverte pluridisciplinaire **HAL**, est destinée au dépôt et à la diffusion de documents scientifiques de niveau recherche, publiés ou non, émanant des établissements d'enseignement et de recherche français ou étrangers, des laboratoires publics ou privés.

Study of the effect of gas pressure and catalyst droplets number density on silicon nanowires growth, tapering, and gold coverage

Cite as: J. Appl. Phys. **107**, 084902 (2010); <https://doi.org/10.1063/1.3359648>

Submitted: 02 November 2009 • Accepted: 09 February 2010 • Published Online: 21 April 2010

W. H. Chen, R. Lardé, E. Cadel, et al.



View Online



Export Citation

ARTICLES YOU MAY BE INTERESTED IN

VAPOR-LIQUID-SOLID MECHANISM OF SINGLE CRYSTAL GROWTH

Applied Physics Letters **4**, 89 (1964); <https://doi.org/10.1063/1.1753975>

Growth of silicon nanowires via gold/silane vapor-liquid-solid reaction

Journal of Vacuum Science & Technology B: Microelectronics and Nanometer Structures Processing, Measurement, and Phenomena **15**, 554 (1997); <https://doi.org/10.1116/1.589291>

Patterned epitaxial vapor-liquid-solid growth of silicon nanowires on Si(111) using silane

Journal of Applied Physics **103**, 024304 (2008); <https://doi.org/10.1063/1.2832760>

Lock-in Amplifiers
up to 600 MHz



Zurich
Instruments



Study of the effect of gas pressure and catalyst droplets number density on silicon nanowires growth, tapering, and gold coverage

W. H. Chen,¹ R. Lardé,¹ E. Cadel,¹ T. Xu,² B. Grandidier,² J. P. Nys,²
D. Stiévenard,² and P. Pareige^{1,a)}

¹*Groupe de Physique des Matériaux, CNRS UMR 6634, Université et INSA de Rouen, Av. de l'université, BP 12, 76801 Saint Etienne du Rouvray, France*

²*Département ISEN, Institut d'Electronique, de Microélectronique et de Nanotechnologie, CNRS UMR 8520, 41 bd Vauban, 59046 Lille Cedex, France*

(Received 2 November 2009; accepted 9 February 2010; published online 21 April 2010)

We investigated the growth of silicon nanowires from Au-rich catalyst droplets by two different methods: chemical vapor deposition (CVD) and molecular beam epitaxy (MBE). The growth rate is found to be diameter-dependent and increases with increasing precursor partial pressures. The comparison of the experimental results with models shows that the contribution of Si atoms that diffuses from the substrate and the NW sidewalls toward the catalyst droplet can be neglected in CVD for the different pressures used in this study, whereas it is the major source of Si supply for the MBE growth. In addition, by decreasing the number density of catalyst droplet prior to the NW growth in CVD, it is also found that this parameter affects the NWs morphology, increasing the tapering effect when the silane partial pressure is small enough to allow gold atom diffusion from the catalyst droplet. © 2010 American Institute of Physics. [doi:10.1063/1.3359648]

I. INTRODUCTION

New materials and evolution of technologies are driving forces for researchers. Among them, silicon nanowires (SiNWs) elaborated by “bottom up” approach are widely studied. Indeed, due to their nanometric size they exhibit new physical properties and could be incorporated in the future Si based technologies,¹ for example, field-effect transistors,² single electron detector³ and biological sensors.⁴ In addition to the nanoelectronic area, other properties of SiNWs are also promising for thermal,⁵ mechanical,⁶ and photovoltaic application.⁷ However, whatever the final application is, the new physical properties of SiNWs need to be identified and understood. In this context, the characterization and understanding of their growth mechanism are of technological and fundamental importance.

There are many methods for growing SiNWs such as chemical vapor deposition (CVD),⁸ laser ablation,⁹ and molecular beam epitaxy (MBE).¹⁰ Although the mechanism of SiNWs growth is still not fully understood, growth models have been developed. Some example (not an exhaustive list) may be found in Refs. 8 and 11–15. Many experimental conditions, for example, the precursor pressure¹⁶ and the size distribution of catalysts,¹⁷ can affect the NW growth rate and morphology simultaneously. However, their relative importance and how they affect the growth rate still need more studies. There are usually two contributions to the growth rate of semiconductor nano wires (NWs): the first one arises from the direct impingement of gas precursors or atoms onto the catalyst droplet, the second one is caused by atoms that adsorb on the substrate or the sidewalls of the NWs and then diffuse to the catalyst droplet. By using a growth model that can account for both contributions, we investigate the depen-

dence of the growth rate as a function of the NW diameter for the case of CVD and MBE. In particular, we show that diffusion can be neglected in CVD, but also that the reason for not considering the Si atom diffusion differs depending on the CVD growth conditions. As far as the morphology of SiNWs is concerned, the tapering effect of SiNWs is a commonly existing phenomenon. Similarly to the need for a better understanding of physical mechanisms involved in the growth rate, it is important to determine what experimental parameters lead to tapered NWs. In this work, we also study the influence of the gas pressure and the catalyst droplet number density on the tapering of the SiNWs.

II. EXPERIMENTAL CONDITION OF SINWS GROWTH

The SiNWs were fabricated by the CVD and MBE method, respectively, using gold droplets as catalyst according to the mechanism of vapor liquid solid (VLS).⁸ In order to obtain gold droplets with different densities, the gold droplets were formed directly by gold deposition on a heated Si(111) surface in ultrahigh vacuum (UHV) or by evaporating a 2 nm thick layer of gold on a H-Si(111) chemically passivated surface. For the process achieved in UHV, two different temperatures were used: 430 °C and 460 °C using the same gold deposition pressure of $8\text{--}8.6 \times 10^{-10}$ mbar. The density and the size (diameter) of the gold droplets are determined by the evaporation flow rate and the temperature of the samples via the Ostwald ripening process. Following these two conditions, two different densities of gold droplets were obtained: at high temperature, the density is lower but the average droplets diameter is larger (55 nm versus 90 nm). Regarding the process of the gold droplet formation from the Au thin film, the sample was annealed at 700 °C for five minute in the CVD chamber prior to NWs growth. Such a

^{a)}Electronic mail: philippe.pareige@univ-rouen.fr.

thermal treatment results in the formation of gold droplets with diameters ranging from 70 nm to a few hundreds of nanometers.

In the next step, the SiNWs were grown by CVD at a temperature of 500 °C for 30 min. Silane was used as the source gas. Under what will be subsequently called a high pressure condition, the source gas, SiH₄, with a flow rate of 50 SCCM (SCCM denotes cubic centimeter per minute at STP), was diluted in a mixture of Ar and H₂ (flow rate of 50 SCCM), to set the pressure in the chamber to 0.8 mbar, the silane partial pressure being 0.4 mbar. In the case of the other growth condition, namely, the low pressure condition, the SiH₄ gas was diluted with H₂ in the ratio 12:150. The flow rate of SiH₄ was 12 SCCM and the total pressure was kept at 1.1 mbar during the NWs growth, yielding a silane partial pressure of 0.08 mbar. In addition, because we need to measure the base diameter of NWs for the growth rate analysis, similar SiNW growths were performed on micropillars, where it is easier to observe a high number density of NWs from the different sideviews. The micropillars were fabricated from Si wafers [111] oriented, n-type doped (0.03–0.05 Ω m), using a standard lithography method.¹⁸ Scanning electron microscopy (SEM) images were performed with a LEO FE 1530 microscope and are shown in Figs. 1(a)–1(c).

As far as the MBE growth of SiNWs is concerned, the catalyst (gold) is deposited on the Si substrate at a temperature of 360 °C. During the growth of the NWs the chamber pressure is kept at a base pressure of 10⁻¹⁰ mbar. The Si atoms are deposited on the Si substrate covered by gold clusters at 550 °C with an evaporation rate of 0.05 nm/s [Fig. 1(d)].

III. RESULTS AND MODEL

A. Results

In the first part of this work, the growth rate of SiNWs fabricated by CVD process is investigated as a function of the gas pressure (silane partial pressure). The growth condition and more precisely the growth rate of SiNWs is one of the first and important parameter for experimental consideration. The growth rate of SiNWs depends on many different experimental parameters such as: temperature, pressure, and flow rate of Si atoms. In addition, the diameter of the gold droplets (or its size distribution) is directly linked to the growth rate. The experimental results showing the variation in the growth rate as a function of the diameter measured at the NW base and the gas pressure is given in Fig. 2 for a growth temperature of 500 °C.

Two comments must be noted. First, for a given growth condition, the growth rate increases with the droplet diameter up to a given diameter and then saturates. The growth rate saturates when the diameter of NWs is about 150 nm at low silane partial pressure and for about 100 nm diameter at high silane partial pressure. Second, for two different conditions of gas pressure, growth rate is more important at high pressure compared to low pressure for a given diameter.

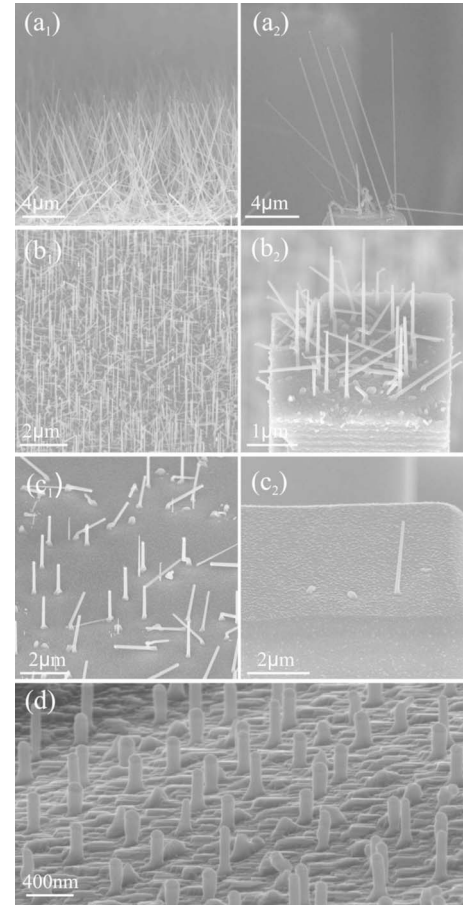


FIG. 1. (a₁), (a₂); (b₁), (b₂) and (c₁), (c₂) SEM images corresponding to the three series of the SiNWs grown on Si substrates and Si pillars, respectively. The silane partial pressure and the average catalyst diameter for growing SiNWs are (a) 0.4 mbar, 55 nm, (b) 0.08 mbar, 55 nm, and 0.08 mbar, (c) 0.08 mbar, and (d) SEM images of SiNWs fabricated by MBE with an evaporation rate 0.05 nm/s.

B. Models

In the typical VLS growing mechanism, and as written by Givargizov,¹¹ the driving force of the growth process of a NW is the difference between the chemical potential of Si in the gas phase and in the crystal phase (NW)

$$\Delta\mu_{\text{Si}} = \mu_{\text{Si}}^{\text{G}} - \mu_{\text{Si}}^{\text{NW}} = \mu_{\text{Si}}^{\text{G}} - \mu_{\text{Si}}^{\text{substrat}} - \frac{4\Omega\gamma}{d}, \quad (1)$$

where $\mu_{\text{Si}}^{\text{j}}$ are the chemical potentials in the gas, NW or substrate. Ω , γ , and d are the specific volume of the atom, the specific surface free energy, and the diameter of the NW, respectively. The chemical potentials of the system are supposed to follow the relation due to the high precursor gas pressure

$$\mu_{\text{Si}}^{\text{sub}} \leq \mu_{\text{Si}}^{\text{NW}} \leq \mu_{\text{Si}}^{\text{L}} \leq \mu_{\text{Si}}^{\text{G}}. \quad (2)$$

In addition, as we intend to characterize the diffusion of Si adatoms from the SiNW sidewalls toward the catalyst droplet, the chemical potential of the Si adatoms has to be considered. If diffusion contributes to the growth rate, then the catalyst droplet will collect the adatoms and this is achieved for

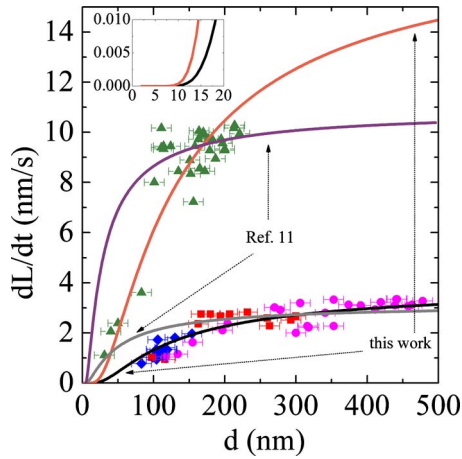


FIG. 2. (Color online) Comparison of growth rates of SiNWs as a function of base diameter for different CVD conditions: same growth temperature but different silane partial pressures. The triangles (\blacktriangle) correspond to a silane partial pressure of 0.4 mbar, whereas the squares (\blacksquare), diamonds (\blacklozenge) and circle (\bullet) correspond to a silane partial pressure of 0.08 mbar. The gold droplets for triangle, square, and diamond conditions are obtained by UHV gold deposition. The density of gold droplets for the triangle and diamond conditions is higher than for the square condition. The gold droplet for the circle condition is obtained by annealing a gold thin film. The curves corresponding to the fit with Givargizov's model (Ref. 11) are indicated. The curves corresponding to the model proposed in this work [Eq. (5)] are also indicated and the zoom for these curves at small diameters is presented in the inset image.

$$\mu_{\text{Si}}^{\text{L}} \leq \mu_{\text{Si}}^{\text{adatom}}. \quad (3)$$

Whatever the process is, CVD or MBE (Si atoms from the decomposition of silane in CVD or the evaporation of Si atoms in MBE), the Au-rich droplet will favor the growth causing the formation of one-dimensional structure. The incorporation will occur either via the droplet surface (interface between gas and liquid) by absorption/desorption mechanisms or via the triple line (gas/liquid/solid line). The Si supersaturation generated in the liquid will induce the crystallization of Si atoms at the liquid/NW interface.

Taking into these mechanisms, the growth rate of a SiNWs could be given by the relation

$$\frac{\pi d^2}{4\Omega} \frac{dL}{dt} = \frac{\pi d^2}{2} A/D + \pi dj, \quad (4)$$

where dL/dt , A/D and j represent the growth rate, the adsorption/desorption part at the droplet surface and the diffusion of Si adatoms from the sidewall toward the droplet/NW interface, respectively. Depending on the growth method, CVD or MBE, the above equation may be simplified.

1. Empirical model for CVD

Considering the CVD fabrication process, the decomposition of silane is needed (not in the case for MBE). This decomposition occurs preferentially at the surface of the catalyst droplet, but can also take place on the NW sidewall depending on the growth conditions. Under low silane partial pressure, we have recently shown that gold atoms diffusing from the Au-rich catalyst droplet toward the NW sidewall can induce faceted sidewalls and form small clusters.¹⁹

These small clusters can act as catalyst droplets to decompose silane, favoring the adsorption of Si atoms on the NW sidewalls. However investigations of the degree of tapering have shown that the Si atoms were directly incorporated into the sidewalls leading to a lateral growth rather than diffusing toward the top Au-rich gold droplet. Because of the roughness of the sidewalls due to the presence of numerous facets, diffusion of Si species is certainly small and thus cannot account for the growth rate of the NWs in CVD.

Under high silane partial pressure, gold atoms were not found to diffuse, except at the end of the NWs that corresponds to the interruption of the gas flow in the growth chamber and the gradual decreases in the Si partial pressure.¹⁹ Indeed due to the high silane partial pressure, the Si dangling bonds are saturated by silane molecules or products of the silane decomposition, preventing gold from diffusing along the surface of the NW shaft.²⁰ As a result, few Si atoms can adsorb on the NW sidewall and their diffusion cannot significantly contribute to the growth rate of the NWs in CVD. Thus, in the CVD process (either at high or low pressure), the sidewall diffusion of Si atoms toward the catalyst droplet can be neglected compared to the direct incorporation of Si atoms into the Au-rich droplet.

An empirical model neglecting the diffusion part has been proposed by Givargizov¹¹ to fit the experimental data in CVD. This empirical expression ($dL/dt \sim (\Delta\mu_{\text{G-S}}/k_{\text{B}}T)^2$) has been used to fit the data set of this present work. The best fit obtained is presented in Fig. 2. It is observed that a good agreement between the experimental data and the model occurs, but only for NWs with large diameters. In this latter growth model, the growth rate was related to the variation in the Si chemical potential between the gas supply phase and the SiNWs. However, the growth rate should be kinetically controlled by the decomposition of silane at the surface of the Au-Si rich droplet, as stated by Wagner.²¹ In such a case, the expression of the growth rate becomes

$$\frac{dL}{dt} = \exp \left[A \left(\frac{\Delta\mu_{\text{Si}}^{\text{G-L}^\infty}}{k_{\text{B}}T} - \frac{4\Omega\gamma_{\text{GL}}}{dk_{\text{B}}T} \right) \right]. \quad (5)$$

One can note that the square exponent is substituted by an exponential expression. The right hand term corresponds to the introduction of Si atoms into the droplet considering the Gibbs-Thomson effect due to the curvature of the droplet surface. L^∞ is a liquid droplet with an infinite radius. In this equation, A is the coefficient of crystallization (nm/s) and $4\Omega\gamma_{\text{GL}}/k_{\text{B}}T$ is related to the Gibbs-Thomson effect. The interfacial energy γ_{GL} for the Au/Si system is assumed to be 0.85 J/m^2 .²²

Under these conditions and hypothesis, the best fit to our experimental data (Fig. 2) is obtained for $A=17 \text{ nm/s}$ and $\Delta\mu_{\text{Si}}^{\text{G-L}^\infty}/k_{\text{B}}T=0.08$ at low silane partial pressure and $A=17 \text{ nm/s}$, $\Delta\mu_{\text{Si}}^{\text{G-L}^\infty}/k_{\text{B}}T=0.17$ at high silane partial pressure. In both cases, A is kept constant because the dominant mechanism for SiNW axial growth rate is the incorporation of Si atoms into the droplet. As the supersaturation is defined by the difference of chemical potential between the gas supply phase and the liquid droplet collector, increasing the gas

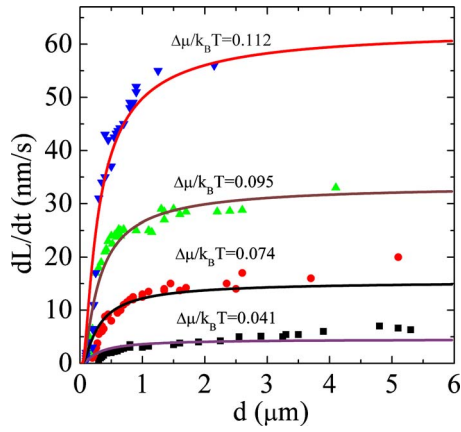


FIG. 3. (Color online) Data extracted from Givargizov's work and fitted with the model presented in this work. These four curves have the same value of $A=37$ nm/s. The supersaturation $\Delta\mu_{\text{Si}}^{\text{G-L}^\infty}/k_B T$ for each condition has the value following: 0.041, 0.074, 0.095, and 0.112.

pressure leads to the increase in the supersaturation, consistent with the variation in $\Delta\mu_{\text{Si}}^{\text{G-L}^\infty}$ deduced from the fitting procedure.

It can be observed, from the fitted curves (inset of Fig. 2), that the NWs can be grown with smaller diameter at high silane pressure compared to low silane partial pressure. At a given growth rate, 0.1 nm/s for example, the diameter of SiNWs grown at high silane pressure is 21 nm compared to 30 nm at low silane pressure, in agreement with the results of Ref. 23.

Comparison of the droplet densities on the growth rate also shows that the density does not affect the growth rate. Indeed, the fitted curve for SiNWs grown at low silane partial pressure overlaps whatever the density of gold droplet at the Si surface prior to the growth of the NWs. Because different droplet density means different average distances between NWs, the diffusion of adatoms from areas between the NWs toward the droplet at the top of the NW shaft can be considered negligible. Therefore, only the incorporation of Si atoms at the droplet surface is predominant.

Our new expression of the growth rate has also been applied to the Givargizov's data extracted from Ref. 11. Figure 3 shows the data sets and the curves using Eq. (5). The coefficient of crystallization A is kept constant to 37 nm/s. It is clearly observed that the growth rate for small and large diameters is well reproduced with our model. The constant growth rate for large diameters strongly supports the hypothesis of the empirical model: the diffusion mechanism may not need to be taken into account. It is consistent with the data of Fig. 2.

2. Diffusion model for MBE

For comparison, the case of SiNWs grown using the MBE process is considered. The growth rate of these SiNWs is reported on Fig. 4(a) as a function of the SiNWs diameter. As expected, the empirical model used for CVD process cannot be applied to reproduce the growth rate trend indicating that the diffusion process cannot be excluded. In the MBE process, the Si atoms flow on droplet and substrate is the same. However the surface of substrate being much larger

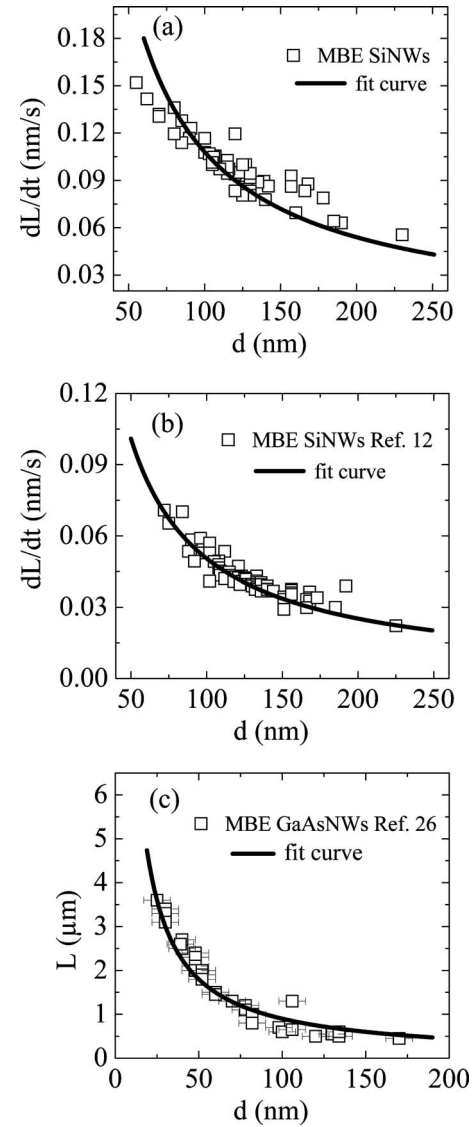


FIG. 4. Evolution of SiNW growth rate under MBE condition. The black fit curve is the model presented in this work. (a) The SiNWs were fabricated by MBE at 550 °C for 60 min. (b) The SiNWs were fabricated by MBE at 525 °C for 240 min (Ref. 12). (c) Case of GaAsNWs grown by MBE (Ref. 26).

than the droplet surface, the A/D term in the Eq. (4) can be neglected. This lead to the expression, derived from Eq. (4)

$$\frac{\pi d^2}{4\Omega} \frac{dL}{dt} = \pi d j. \quad (6)$$

The diffusion flux can be written as a Nernst–Einstein's diffusion flux expression²⁴

$$j = - \frac{nD}{k_B T} \frac{\partial \mu}{\partial L} \quad (7)$$

As a result, the growth rate expression has a form following:

$$\frac{dL}{dt} = \frac{4\Omega}{d} \times \frac{nD}{k_B T} \times \frac{\Delta\mu_{\text{Si}}^{\text{adatom-L}}}{\lambda_{\text{NW}}}. \quad (8)$$

The right term corresponds to the diffusion of Si adatoms from the sidewall of the SiNW toward the triple line. $\Delta\mu_{\text{Si}}^{\text{adatom-L}}$ is the difference in chemical potential between

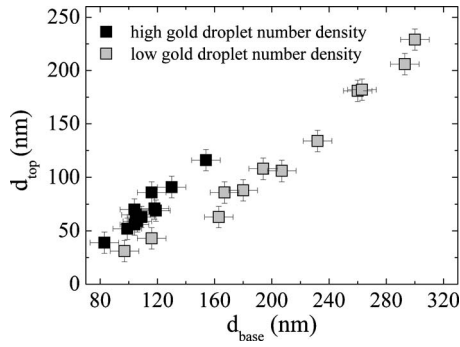


FIG. 5. Measurements of the top diameters (d_{top}) of the SiNWs as a function of their base diameters (d_{base}). Measurements from the high density droplets are reported in black squares and from low density droplets in gray squares.

the adatoms at the SiNWs surface and the triple line. n is the Si adatom density on the NW sidewall. It will be taken here as its maximum value, namely one monolayer. D and λ_{NW} are the diffusion coefficient and the effective diffusion length of Si adatoms on the NW sidewall. The experimental data were collected from the SiNWs fabricated by MBE. The growth temperature and growth time is 500 °C and 60 min, respectively. The values of D and λ_{NW} , following Ref. 25, are estimated to be about 10^{-10} cm²/s and 1 μ m, respectively, and $\Delta\mu_{Si}^{G-L}/k_B T=1$. As shown in Fig. 4(a), the growth rate of SiNWs decreases with the increase in diameter and a good agreement is observed between experimental data and the curve from Eq. (8). In order to test Eq. (8), SiNWs experimental data from Ref. 12 are also reported in Fig. 4(b). The values of D and λ_{NW} were chosen to be 4.1×10^{-11} cm²/s and 0.9 μ m, respectively, because of the lower temperature 525 °C compared to our growth temperature (550 °C). It should be noted that both experimental conditions have the same deposition flux 0.05 nm/s. Thus $\Delta\mu_{Si}^{G-L}/k_B T$ is changed only with temperature and is chosen to be 1.03 correspondently. This diffusion model is also valid for the MBE growth of III-V NWs such as GaAsNWs. Indeed, it fits the experimental data of GaAsNWs from Dubrovskii' group,²⁶ as shown in Fig. 4(c).

C. Effect of growth conditions on tapering of SiNWs

Two reasons can contribute to the tapering phenomenon of SiNWs: the decrease in diameter of the catalyst droplet²⁷ and/or the lateral growth of SiNW.¹⁹ In most technological cases this phenomenon must be avoided in order to have NWs with uniform diameter. It is thus important to understand the physical mechanisms that lead to the tapering effect.

1. Effect of the number density of gold droplets on tapering

In this part, the influence of the gold droplet density on the tapering effect is considered. The SiNWs were grown with two different densities of gold droplet under the same low pressure and temperature. The results are reported in Fig. 5. A linear behavior is found between the diameter d_{top} of the droplet at the top of the NWs and the diameter d_{base} of their base. The slopes of both sets of data are identical. This

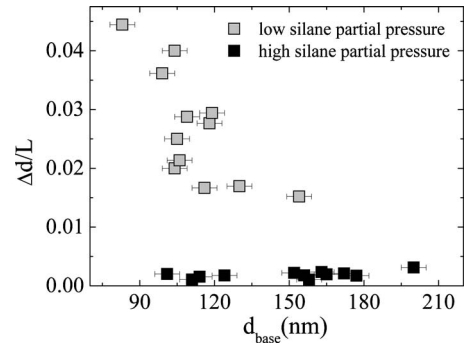


FIG. 6. Degree of tapering, defined as $\Delta d/L=(d_{base}-d_{top})/L$, as a function of the NW diameter for two different silane partial pressures. d_{base} and d_{top} are, respectively, the base and the top diameters of the SiNWs and L their length.

indicates that the mechanism at the origin of the tapering effect is the same for both conditions, namely, the reduction in Au-rich droplets and the lateral growth. It must be noted that in the case of the growth conditions used in this work, the desorption of gold atoms from the droplet to the gas phase can be neglected, as indicating in Ref. 28. Therefore, the reduction in the Au-rich droplet size is only related to diffusion of gold atoms from the droplet toward the NW sidewalls. Remarkably, although the growth conditions are the same, the tapering effect is more pronounced in the case of the low density of droplets, when NWs with a similar base diameter are considered. The reason will be discussed afterwards.

2. Effect of silane partial pressure on tapering of SiNWs

In this part, the effect of the silane partial pressure on the tapering effect is considered. SiNWs were grown under two different pressures but with the same temperature (500 °C), growth time (30 min) and density of Au-rich droplets. The average tapering quantity corresponds to the decrease in the diameter along the main axis of the NW. It is defined as $(d_{base}-d_{top})/L=\Delta d/L$. As the ratio between Δd and L is small, it corresponds to the angle between the main axis of the NW and the segment defined by the NW sidewall. The top and base diameters of the SiNWs and their length were measured with SEM. The results are reported in Fig. 6. At low silane partial pressure, it clearly appears that the tapering varies as the inverse of the length. Indeed, the rate of the lateral growth can be considered constant for a given sample. As discussed above, the dissociation of silane at the NW sidewall does not lead to a diffusion of the Si atoms toward the Au-rich droplet, but rather to their direct incorporation to the sidewall, causing lateral overgrowth. If we assume that all the NWs start to grow at the same time, the quantity of lateral overgrowth will be the same whatever their initial diameter at a given length from the NW basis. Since the thickness of the Si layer overgrown on the Si sidewall along the main axis of the wire depends only on the duration of the growth and NWs with the bigger diameters have the higher growth rate, the tapering angle will decrease as $1/L$ as the total diameter increases. In contrast, at high silane partial

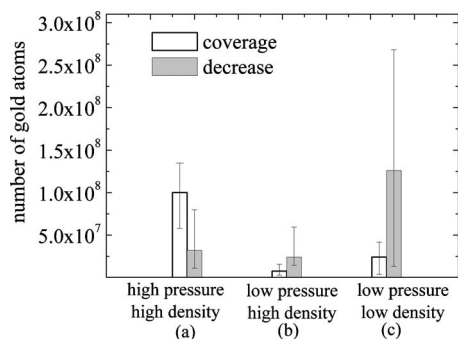


FIG. 7. Average gold atoms variation in droplets compared to average gold atoms needed to cover the sidewall surface for three different growth conditions. White and gray bars represent the gold atom coverage on the SiNW sidewall surface and the reduction in gold atoms in the droplet during the SiNW growth, respectively, for all three growth conditions. Error bars represent the deviation obtained from 12 samples.

pressure, the ratio between Δd and L is quite small and does not significantly vary with as the total diameter of the NWs increases.

It must be noted that the difference in the $\Delta d/L$ values, for a given SiNW diameter, when both effects, density/pressure, are compared, is ten times much greater in the case of a change in the silane pressure. This clearly indicates that the effect of silane partial pressure is more significant on tapering effect than the catalyst droplets density.

3. Discussion

As mentioned earlier, two reasons are at the origin of the tapering effect: droplet size reduction and lateral growth. This first part of discussion focuses on the gold atoms reduction in droplets. The reason for the reduction in droplet size is the diffusion of gold atoms from droplet along the NW sidewall. It has been shown in Ref. 27 that the diffusion of gold atoms from the droplet toward the NW sidewall surface is the major mechanism for tapering during growth. The evolution of the number of gold atoms diffusing from the droplet toward the sidewall may be estimated depending on the growing conditions. In order to do this, the gold droplet is assumed to be half a sphere, the contact angle of the droplet being 90° . Also, it is supposed that the droplet is of pure gold at the beginning of the growth and that the gold concentration at the end of the growth may be given by the Au/Si phase diagram.²⁹

Although the initial diameter of the Au-rich droplet is not known, we measured the top and base diameters and first assume that the base diameter does not change during the growth. As a result, the reduction in the droplet size can be measured from the difference between the base diameter compared to the top diameter. For comparison, we calculate the number of gold atoms required to wet the NW sidewall with one monolayer.²⁷ As this wetting layer is supplied by the Au-rich droplet at the top of the NWs, it should be related to the decrease in size of the droplet. Figure 7 shows the comparison between both quantities and the plotted data correspond to the average values obtained for 12 different NWs and the three different growth conditions.

It is clearly shown in the case of the high silane partial pressure [Fig. 7(a)], that the lost of gold atoms in droplets is not sufficient to cover the entire sidewall surface. As stated previously, a high silane partial pressure results in saturation of the atomic sites on the SiNWs sidewalls inhibiting the gold diffusion process. Thus we were not able to detect a significant tapering effect at high silane partial pressure. However, the reverse situation is observed when the silane partial pressure is low and whatever the number densities of droplets are [Figs. 7(b) and 7(c)]. It can be assumed in these later cases that gold diffusion occurs on the NW sidewall as well as lateral growth. Owing to these considerations, the results presented in Figs. 5 and 6 can be discussed.

At low silane partial pressure, the lateral growth contribution to tapering of NWs can be assumed to be identical because experimental conditions (same total pressure, same silane partial pressure and same temperature) are the same. However, Fig. 5 shows that the NWs prepared with the lower density of droplet are more tapered. Therefore, this variation in the tapering effect is only caused by the diffusion of gold atoms on the NW sidewalls. It must be noted here that the total number of gold atoms deposited on the Si substrates, prior to SiNWs growth, has the same value because gold deposition flux and time were the same for both samples. Before NWs growth start, the regions between the droplets show the same atomic reconstruction: a Au/Si(111)-($\sqrt{3} \times \sqrt{3}$) phase.¹⁸ The Gibbs–Wulff theory indicates that the gradient of chemical potential is the driving force for diffusion on surface.²⁵ In our case, the diffusion coefficient of gold atoms on all NW surfaces has the same value because the pressure and the temperature are identical for both samples. The gold atoms flow on NW sidewall surface, j , can be given by the relation of Nernst–Einstein [Eq. (7)]. As the gold atom density on the surface is small, then gold diffuses from the droplets toward the regions of the substrate located between the NWs. Because these regions are bigger in the case of a sample with a low density of droplets, they can accommodate more Au adatoms diffusing from the droplets during the growth. These droplets thus lose more gold atoms, causing the formation of NWs that are more tapered.

Finally, we have shown in this work, Fig. 1, that the growth direction of SiNWs will change from [111] to [112] for relatively large SiNWs diameters when the silane partial pressure changes from low (0.08 mbar) to high (0.4 mbar), in agreement with Ref. 30. Thus the optimized growing condition to avoid tapering effect and change in crystallographic direction consists in using a moderate silane partial pressure with a high total gas pressure.

IV. CONCLUSION

In this work, detailed analyses of the lengths and diameters of SiNWs grown either by CVD or by MBE allow to determine how variations in the NW diameter modify the growth rate and the morphology of the NWs. For the CVD growth, an empirical model is proposed, where the growth results from the Si species decomposed at the surface of the catalyst droplet and the subsequent condensation of the Si atoms at the interface between the Au-rich droplet and the

SiNW shaft. On the contrary, the growth in MBE is predominantly related to the diffusion of Si atoms from the substrate. Finally, in CVD, while the density of gold droplets is not involved in the growth rate of the NWs, we have found that it affects the degree of NW tapering, a high density of droplets before growth leading to a reduction in the tapering effect. These observations are important for the optimization and control of the growth of SiNWs and to avoid gold diffusion at the SiNWs surface.

ACKNOWLEDGMENT

We thank the DGA (Direction Générale de l'Armement) which partly supports this work under the contract REI-N02008.34.0031.

- ¹M. H. Huang, S. Mao, H. Feick, H. Yan, Y. Wu, H. Kind, E. Weber, R. Russo, and P. Yang, *Science* **292**, 1897 (2001).
- ²Y. Cui, Z. Zhong, D. Wang, W. U. Wang, and C. M. Lieber, *Nano Lett.* **3**, 149 (2003).
- ³J.-i. Hahm and C. M. Lieber, *Nano Lett.* **4**, 51 (2004).
- ⁴Y. Cui, Q. Wei, H. Park, and C. M. Lieber, *Science* **293**, 1289 (2001).
- ⁵D. Li, Y. Wu, R. Fan, P. Yang, and A. Majumdar, *Appl. Phys. Lett.* **83**, 3186 (2003).
- ⁶R. He and P. Yang, *Nat. Nanotechnol.* **1**, 42 (2006).
- ⁷B. Tian, X. Zheng, T. J. Kempa, Y. Fang, N. Yu, G. Yu, J. Huang, and C. M. Lieber, *Nature (London)* **449**, 885 (2007).
- ⁸R. S. Wagner and W. C. Ellis, *Appl. Phys. Lett.* **4**, 89 (1964).
- ⁹A. M. Morales and C. M. Lieber, *Science* **279**, 208 (1998).
- ¹⁰J. L. Liu, S. J. Cai, G. L. Jin, S. G. Thomas, and K. L. Wang, *J. Cryst. Growth* **200**, 106 (1999).
- ¹¹E. I. Givargizov, *J. Cryst. Growth* **31**, 20 (1975).
- ¹²L. Schubert, P. Werner, N. D. Zakharov, G. Gerth, F. M. Kolb, L. Long, U. Gosele, and T. Y. Tan, *Appl. Phys. Lett.* **84**, 4968 (2004).
- ¹³Z. Chen and C. Cao, *Appl. Phys. Lett.* **88**, 143118 (2006).
- ¹⁴V. G. Dubrovskii, N. V. Sibirev, G. E. Cirlin, I. P. Soshnikov, W. H. Chen, R. Larde, E. Cadel, P. Pareige, T. Xu, B. Grandidier, J. P. Nys, D. Stievenard, M. Moewe, L. C. Chuang, and C. Chang-Hasnain, *Phys. Rev. B* **79**, 205316 (2009).
- ¹⁵V. Schmidt, J. V. Wittemann, S. Senz, and U. Gösele, *Adv. Mater.* **21**, 2681 (2009).
- ¹⁶H. Zhao, S. Zhou, Z. Hasanali, and D. Wang, *J. Phys. Chem. C* **112**, 5695 (2008).
- ¹⁷S. T. Boles, E. A. Fitzgerald, C. V. Thompson, C. K. F. Ho, and K. L. Pey, *J. Appl. Phys.* **106**, 044311 (2009).
- ¹⁸T. Xu, J. P. Nys, B. Grandidier, D. Stievenard, Y. Coffinier, R. Boukherroub, R. Larde, E. Cadel, and P. Pareige, *J. Vac. Sci. Technol. B* **26**, 1960 (2008).
- ¹⁹T. Xu, J. P. Nys, A. Addad, O. I. Lebedev, A. Urbietta, B. Salhi, M. Berthe, B. Grandidier, and D. Stievenard, *Phys. Rev. B* **81**, 115403 (2010).
- ²⁰M. I. den Hertog, J.-L. Rouviere, F. Dhalluin, P. J. Desré, P. Gentile, P. Ferret, F. Oehler, and T. Baron, *Nano Lett.* **8**, 1544 (2008).
- ²¹R. S. Wagner, *J. Appl. Phys.* **38**, 1554 (1967).
- ²²N. Li, T. Y. Tan, and U. Gösele, *Appl. Phys. A: Mater. Sci. Process.* **86**, 433 (2007).
- ²³F. Dhalluin, P. J. Desre, M. I. den Hertog, J.-L. Rouviere, P. Ferret, P. Gentile, and T. Baron, *J. Appl. Phys.* **102**, 094906 (2007).
- ²⁴M. Z. A. Munshi, *Handbook of Solid State Batteries and Capacitors* (World Scientific, Singapore, 1995), Vol. 16.
- ²⁵A. Pimpinelli and J. Villian, *Physics of Crystal Growth* (Cambridge University Press, Cambridge, 1998).
- ²⁶V. G. Dubrovskii, G. E. Cirlin, I. P. Soshnikov, A. A. Tonkikh, N. V. Sibirev, Y. B. Samsonenko, and V. M. Ustinov, *Phys. Rev. B* **71**, 205325 (2005).
- ²⁷J. B. Hannon, S. Kodambaka, F. M. Ross, and R. M. Tromp, *Nature (London)* **440**, 69 (2006).
- ²⁸L. Cao, B. Garipcan, J. S. Atchison, C. Ni, B. Nabet, and J. E. Spanier, *Nano Lett.* **6**, 1852 (2006).
- ²⁹E. J. Schwalbach and P. W. Voorhees, *Nano Lett.* **8**, 3739 (2008).
- ³⁰Y. Wu, Y. Cui, L. Huynh, C. J. Barrelet, D. C. Bell, and C. M. Lieber, *Nano Lett.* **4**, 433 (2004).